Structural Analysis of F/OH Distribution in a Hybrid Open-Framework Fluorinated Gallium Oxalate−Phosphate Templated by 1,3-Diaminopropane (MIL-90)

Thierry Loiseau,*,† Gérard Férey,†,‡ Mohamed Haouas,† and Francis Taulelle†

Institut Lavoisier (UMR CNRS 8637) and Institut Universitaire de France, Université de Versailles St Quentin en Yvelines, 45, Avenue des Etats Unis, 78035 Versailles, France

Received July 20, 2004. Revised Manuscript Received September 17, 2004

A new gallium oxalate−phosphate compound MIL-90 or $Ga_5(PO_4)_4(C_2O_4)F_2(OH)_2 \cdot 1.5N_2C_3H_{12}$ was synthesized under mild hydrothermal conditions (180 °C, 24 h) by using 1,3-diaminopropane as a structure-directing agent. Its structure was characterized by means of single-crystal XRD analysis and multinuclear solid state NMR; it consists of the corner-shared connection of PO_4, GaO_4 tetrahedra with GaO_5X and GaO_2X_4 octahedra where X = OH or F. ^{19}F and ^{31}P MAS NMR showed statistical distribution of the fluorine and hydroxyl group on the bridging sites between the two types of the octahedrally coordinated gallium atoms. ^{71}Ga MAS NMR indicated two different kinds of gallium within the structure, with tetrahedral and octahedral environment. The gallium octahedra $GaO_5F_x(OH)_{1-x}$ ($x \approx 0.72$) are linked together through the oxalate anions, which results in the formation of a layerlike structure comprising the oxalate bridging dimer of $GaO_5F_x(OH)_{1-x}$ ($x \approx 0.72$) and GaO_4 tetrahedra connected to the phosphate anions. The resulting sheets are stacked along the *c* axis and connected to each other via the GaO_2X_4 (X = OH or F) octahedra. This specific arrangement generates a three-dimensional framework with intersecting channels bound by 10 polyhedra (4.5 × 4.5 Å) running along [100] and [010]. Within the tunnels are located the diprotonated 1,3-diaminopropane species, confirmed by ^1H MAS and ^{13}C CPMAS experiments, which preferentially interact via hydrogen bond with the terminal fluorine or hydroxyl group of gallium octahedra GaO_2X_4 (X = OH or F). Crystal data for $Ga_5(PO_4)_4(C_2O_4)F_2(OH)_2 \cdot 1.5N_2C_3H_{12}$: $a = 8.1217(6)$ Å, $b = 8.9601(6)$ Å, $c = 10.4611(8)$ Å, $\alpha = 111.930(1)°$, $\beta = 103.655(1)°$, $\gamma = 101.903(1)°$, $V = 648.59(8)$ Å^3, $P\bar{1}$ (No. 2), $Z = 1$, R1 = 0.0598, wR2 = 0.1568 for 3247 reflections $I > 2\sigma(I)$.

Introduction

Since the discovery of the microporous aluminum phosphates, the hydrothermal preparation and structural characterization of new open-framework solids templated by organic molecules (amines, etc.) were intensively investigated. Following the synthesis strategy initiated by Flanigen and co-workers,[1] a wide variety of phosphate-based solids was obtained including heavier group 13 elements (Ga, In, etc.) or transition metals replacing aluminum in the inorganic framework.[2] In some cases, literature reported the characterization of extra-large-pore three-dimensional networks with systems of tunnels delimited by 24 cations (gallium phosphate,[3] zinc phosphate ND-1,[4] nickel phosphate VSB-1[5] and VSB-5[6]). Recently, several works have focused on the use of multidentate carboxylate-based ligands associated with the phosphate anion, resulting in the formation of porous organic−inorganic hybrid materials. Among the large number of carboxylates compounds, the oxalate moiety, $C_2O_4^{2-}$, was found to be a good candidate[7] and has been successfully incorporated into phosphates frameworks with the different metals such as V,[8−11] Fe,[12−17] Co,[18] Zn,[19] Al,[20−22] Ga,[23−27] and In.[28] In these phases, the oxalate

* To whom correspondence should be addressed. E-mail: loiseau@chimie.uvsq.fr. Phone: 33 1 39 254 373. Fax: 33 1 39 254 358.

† Institut Lavoisier (UMR CNRS 8637).

‡ Institut Universitaire de France.

(1) Wilson, S. T.; Lok, B. M.; Messina, C. A.; Cannan, T. R.; Flanigen, E. M. *J. Am. Chem. Soc.* **1982**, *104*, 1146.

(2) Cheetham, A. K.; Férey, G.; Loiseau, T. *Angew. Chem., Int. Ed.* **1999**, *38*, 3268.

(3) Lin, C.-H.; Wang, S.-L.; Lii, K.-H. *J. Am. Chem. Soc.* **2001**, *123*, 4649.

(4) Yang, G.-Y.; Sevov, S. C. *J. Am. Chem. Soc.* **1999**, *121*, 8389.

(5) Guillou, N.; Gao, Q.; Noguès, M.; Morris, R. E.; Hervieu, M.; Férey, G.; Cheetham, A. K. *C. R. Acad. Sci. Paris* **1999**, *2*, 387.

(6) Guillou, N.; Gao, Q.; Forster, P. M.; Chang, J.-S.; Noguès, M.; Park, S.-E.; Férey, G.; Cheetham, A. K. *Angew. Chem., Int. Ed.* **2001**, *40*, 2831.

(7) Rao, C. N. R.; Natarajan, S.; Choudhury, A.; Neeraj, S.; Vaidhyanathan, R. *Acta Crystallogr. B* **2001**, *57*, 1.

(8) Tsai, Y.-M.; Wang, S.-L.; Huang, C.-H.; Lii, K.-H. *Inorg. Chem.* **1999**, *38*, 4183.

(9) Do, J.; Bontchev, R. P.; Jacobson, A. J. *Inorg. Chem.* **2000**, *39*, 3230.

(10) Do, J.; Bontchev, R. P.; Jacobson, A. J. *Chem. Mater.* **2001**, *13*, 2601.

(11) Tang, M.-F.; Lii, K.-H. *J. Solid State Chem.* **2004**, *177*, 1912.

(12) Choudhury, A.; Natarajan, S.; Rao, C. N. R. *J. Solid State Chem.* **1999**, *146*, 538.

(13) Choudhury, A.; Natarajan, S. *J. Mater. Chem.* **1999**, *9*, 3113.

(14) Choudhury, A.; Natarajan, S.; Rao, C. N. R. *Chem. Mater.* **1999**, *11*, 2316.

(15) Lin, H.-M.; Lii, K.-H.; Jiang, Y.-C.; Wang, S.-L. *Chem. Mater.* **1999**, *11*, 519.

(16) Chang, W.-J.; Lin, H.-M.; Lii, K.-H. *J. Solid State Chem.* **2001**, *157*, 233.

10.1021/cm048820o CCC: $27.50
Published on Web 11/09/2004

anion usually acts as a bridging ligand between two metallic centers and this led to the design of novel class of hybrid networks.

As part of our general exploration, we concentrated our efforts on the synthesis of organically templated gallium phosphates incorporating fluoride anions.[29] Flanigen's fluoride method[30,31] was extensively applied for the formation of porous materials and appeared very promising in the gallium system. Several solids containing very open three-dimensional frameworks have been thus described in the GaPOF series (Cloverite,[32] MIL-46,[33] MIL-31,[34] and MIL-50[35]).

In this contribution, we first attempted the synthesis of mixed gallium phosphate−oxalate compound synthesized in the presence of fluorine. The reactivity of the molecule 1,3-diaminopropane as a structure-directing agent was considered in this work. This organic molecule was previously used for structure-directing the fluorinated gallium phosphate networks ULM-3[36] and ULM-4.[37] Here we report the structural effect of the addition of oxalic acid in hydrothermal reaction medium in the GaPOF system. With 1,3-diaminopropane, the novel phase MIL-90 or $Ga_5(PO_4)_4(C_2O_4)F_2(OH)_2 \cdot 1.5N_2C_3H_{12}$ is obtained and its structure exhibits an open-framework based on channels bound by 10 polyhedra (PO_4, GaO_4, GaO_5X, or GaO_2X_4, X = OH or F) encapsulating the organic species. In this paper, the synthesis, crystal structure, and solid-state NMR (^1H, ^{13}C, ^{31}P, ^{71}Ga) of MIL-90 are presented.

Experimental Section

The title compound MIL-90 or $Ga_5(PO_4)_4(C_2O_4)F_2(OH)_2 \cdot 1.5N_2C_3H_{12}$ was prepared by hydrothermal method under autogenous pressure. The reactants were gallium oxide (Ga_2O_3, Aldrich, 99.99%+), phosphoric acid (85% H_3PO_4, Prolabo, RP Normapur), hydrofluoric acid (40% HF, Prolabo RP Normapur), oxalic acid ($HO_2C-CO_2H \cdot 2H_2O$, Alfa, noted *ox*) and 1,3-diaminopropane ($H_2N-(CH_2)_3-NH_2$, Aldrich, 99%+, noted *dap*). *HF is a hazardous acid which must be handled with care*. The starting mixture, corresponding to the molar composition 1 Ga_2O_3 (650 mg), 2 H_3PO_4 (0.47 mL), 2 HF (0.29 mL), 2 *ox* (874.5 mg), 0.8 *dap* (0.24 mL), and 80 H_2O (5 mL), was placed in a Teflon-lined stainless steel autoclave, heated at 180 °C for 24 h, and then cooled to room temperature for 12 h. The pH of the synthesis medium was 1 at the end of the hydrothermal treatment. The obtained white crystalline product was collected by filtration, washed with distilled water, and dried at room temperature. The powder X-ray diffraction pattern indicated that the product was a new compound.

Ga, P, F, N, and C chemical analyses were performed at the National Center of Analysis of CNRS (Vernaison, France). The elemental analysis of the sample gave the following results according to the chemical formula of the title compound $Ga_5(PO_4)_4(C_2O_4)F_2(OH)_2 \cdot 1.5N_2C_3H_{12}$ (weight %): Ga, 35.0 (calc. 34.8); P, 12.5 (calc. 12.4); F, 3.6 (calc. 3.8); N, 3.5 (calc. 4.2); C, 7.1 (calc. 7.8).

Thermogravimetry analysis was carried out on a TA Instrument type 2050 thermoanalyzer under nitrogen gas flow with a heating rate of 2 °C·min^{-1}. The TG curve shows two events between 25 and 800 °C. The first mass loss (6.1%) is observed between room temperature and 280 °C and could be assigned to the partial removal of terminal and bridging species OH and F (calc: 7.1%) linked to gallium atoms. The second weight loss (15.5%) occurring between 330 and 650 °C is attributed to the departure of the amine molecule (calc: 14.0%) together with the collapse of the structure. The powder XRD pattern of the residue at 800 °C indicated that the product is amorphous.

Single-Crystal XRD Analysis. The structure of MIL-90 was determined by means of single-crystal X-ray diffraction analysis. A platelet-shaped crystal was carefully selected under a polarizing microscope and glued to the top of a thin glass fiber with Araldite adhesive. The intensity data were recorded on a Siemens SMART three-circle diffractometer equipped with a CCD bidimensional detector (molybdenum radiation). The crystal-to-detector distance was 45 mm allowing for the data collection up to 60° (2θ). Slightly more than one hemisphere of data was recorded and the acquisition time per frame was 30 s with a scan width of 0.3° in ω. An empirical absorption correction was applied using the SADABS[38] program. The structure of MIL-90 was solved by direct methods in the centric space group $P\bar{1}$ (No. 2) and refined by full-matrix least squares using the SHELXTL[39] package. The gallium and phosphorus atoms were located by direct methods and all the other non-hydrogen atoms (F, O, C, N) were placed from subsequent Fourier-difference map calculations. The location of the fluorine atom on the site F1 was deduced from the analysis of the anisotropic thermal parameters and bond valence calculations. It is in agreement with the fluorine content obtained from the chemical elemental analysis (with a P/F ratio of ~2). One of the oxygen atoms O9 corresponds to a hydroxyl group and is engaged in a terminal Ga−OH bonding with the gallium Ga3. The positioning of the propanediammonium species within the pores was difficult because of the partial occupancy together with possible disorder of the atoms of the diamine. In agreement with the chemical analysis, the occupancy factors of nitrogen and carbon atoms were fixed to 75%. Distances constraints were applied in order to get a realistic model for the organic molecule. The final refinement converged at R1 = 0.0598, wR2 = 0.1568 for 3247 reflections $I > 2\sigma(I)$. Crystal data and details of the data collection are summarized in Table 1. The resulting atomic coordinates are listed in Table 2.

(17) Jiang, Y.-C.; Wang, S.-L.; Lee, S.-F.; Lii, K.-H. *Inorg. Chem.* **2003**, *42*, 6154.
(18) Choudhury, A.; Natarajan, S. *Solid State Sci.* **2000**, *2*, 365.
(19) Neeraj, S.; Natarajan, S.; Rao, C. N. R. *J. Chem. Soc., Dalton Trans.* **2001**, 289.
(20) Lightfoot, P.; Lethbridge, Z. A. D.; Morris, R. E.; Wragg, D. S.; Wright, P. A. *J. Solid State Chem.* **1999**, *143*, 74.
(21) Kedarnath, K.; Choudhury, A.; Natarajan, S. *J. Solid State Chem.* **2000**, *150*, 324.
(22) Rajic, N.; Logar, N. Z.; Mali, G.; Kaucic, V. *Chem. Mater.* **2003**, *15*, 1734.
(23) Chen, C.-Y.; Chu, P. P.; Lii, K.-H. *Chem. Commun.* **1999**, 1473.
(24) Hung, L.-C.; Kao, H.-M.; Lii, K.-H. *Chem. Mater.* **2000**, *12*, 2411.
(25) Lii, K.-H.; Chen, C.-Y. *Inorg. Chem.* **2000**, *39*, 3374.
(26) Choi, C. T. S.; Anokhina, E. V.; Day, C. S.; Zhao, Y.; Taulelle, F.; Huguenard, C.; Gan, Z.; Lachgar, A. *Chem. Mater.* **2002**, *14*, 4096.
(27) Mrak, M.; Kolitsch, U.; Lengauer, C.; Kaucic, V.; Tillmanns, E. *Inorg. Chem.* **2003**, *42*, 598.
(28) Huang, C.-H.; Lii, K.-H. *J. Chem. Soc., Dalton Trans.* **1998**, 4085.
(29) Loiseau, T.; Férey, G. *J. Chem. Soc., Chem. Commun.* **1992**, 1197.
(30) Flanigen, E. M.; Patton, R. L. U.S. Patent 4,073,865, 1978.
(31) Guth, J. L.; Kessler, H.; Wey, R. *Stud. Surf. Sci. Catal.* **1986**, *28*, 121.
(32) Estermann, M.; McCusker, L. B.; Baerlocher, C.; Merrouche, A.; Kessler, H. *Nature* **1991**, *352*, 320.
(33) Sassoye, C.; Marrot, J.; Loiseau, T.; Férey, G. *Chem. Mater.* **2002**, *14*, 1340.
(34) Sassoye, C.; Loiseau, T.; Taulelle, F.; Férey, G. *Chem. Commun.* **2000**, 943.
(35) Beitone, L.; Marrot, J.; Loiseau, T.; Férey, G.; Henry, M.; Huguenard, C.; Gansmüller, A.; Taulelle, F. *J. Am. Chem. Soc.* **2003**, *125*, 1912.
(36) Loiseau, T.; Retoux, R.; Lacorre, P.; Férey, G. *J. Solid State Chem.* **1994**, *111*, 427.
(37) Loiseau, T.; Taulelle, F.; Férey, G. *Microporous Mater.* **1997**, *9*, 83.
(38) Sheldrick, G. M. *SADABS, a Program for the Siemens Area Detector ABSorption Correction*; University of Göttingen, Germany, 1995.
(39) Sheldrick, G. M. *SHELXTL version 5.03, Software Package for Crystal Structure Determination*; University of Göttingen, Germany, 1994.

Table 1. Crystal Data and Structure Refinement for MIL-90

identification code	MIL-90
empirical formula	$Ga_{2.50}P_2O_{11}FN_{1.50}C_{3.25}H_{2.75}$
formula weight	494.06
temperature	293(2) K
wavelength	0.71073 Å
crystal system, space group	triclinic, $P\bar{1}$
unit cell dimensions	a = 8.1217(6) Å; α = 111.930(1)°
	b = 8.9601(6) Å; β = 103.655(1)°
	c = 10.4611(8) Å; γ = 101.903(1)°
volume	648.59(8) Å^3
Z, calculated density	2, 2.530 Mg/m^3
absorption coefficient	5.488 mm^{-1}
F(000)	475
crystal size	0.240 × 0.08 × 0.03 mm
theta range for data collection	2.24 to 29.73°
limiting indices	$-10 \le h \le 11$, $-12 \le k \le 11$, $-14 \le l \le 12$
reflections collected/unique	4604/3247 [R(int) = 0.0340]
completeness to theta = 29.73	87.9%
refinement method	full matrix least squares on F^2
data/restraints/parameters	3247/7/181
goodness of fit on F^2	1.018
final R indices [$I > 2\sigma(I)$]	R1[a] = 0.0598, wR2[b] = 0.1568
R indices (all data)	R1[a] = 0.0764, wR2[b] = 0.1654
extinction coefficient	0.006(2)
largest diff. peak and hole	2.603 and −1.979 e.Å^{-3}

[a] $R1 = \sum||F_o| - |F_c||/\sum|F_o|$. [b] $WR2 = \{\sum[w(|F_o|^2 - |F_c|^2)^2]/\sum[w(|F_o|^2)^2]\}^{1/2}$, $w = 1/[\sigma^2(F_o^2) + (0.1042P)^2]$ where $P = [(F_o^2) + 2F_c^2]/3$.

Table 2. Atomic Coordinates (× 10^4) and Equivalent Isotropic Displacement Parameters (Å^2 × 10^3) for MIL-90

	x	y	z	U(eq)[a]
Ga1	1986(1)	3517(1)	3630(1)	12(1)
Ga2	7235(1)	9(1)	4469(1)	13(1)
Ga3	0	0	0	16(1)
P1	5492(2)	2743(2)	5164(2)	13(1)
P2	9909(2)	−298(2)	2912(2)	12(1)
F1	1449(5)	2270(5)	1580(4)	19(1)
O1	−319(6)	4086(6)	3139(5)	18(1)
O2	6784(6)	4429(6)	6417(5)	18(1)
O3	2094(6)	4835(6)	5703(5)	16(1)
O4	4102(6)	2945(6)	4065(5)	20(1)
O5	10531(7)	1615(6)	3744(5)	21(1)
O6	8061(6)	−989(6)	3001(6)	22(1)
O7	6503(6)	1741(6)	4280(5)	17(1)
O8	4713(7)	1733(6)	5912(6)	22(1)
O9	2134(7)	−536(6)	−38(6)	23(1)
O10	9782(8)	−1004(6)	1321(5)	25(1)
O11	11203(7)	−1011(6)	3666(6)	24(1)
C1	−693(8)	4778(8)	4255(7)	14(1)
N1	5464(14)	1967(13)	1374(11)	39(2)
C2	4940(30)	3150(30)	680(20)	112(8)
C3	5620(30)	2960(40)	−600(30)	188(16)
C4	7660(30)	3930(50)	−20(30)	184(15)
N2	8495(19)	3727(18)	−1126(15)	67(4)

[a] U(eq) is defined as one-third of the trace of the orthogonalized U_{ij} tensor.

Solid State NMR. NMR spectra were acquired on a Bruker Avance 500 spectrometer with a 11.7 T field, equipped with Bruker MAS 4-mm and 2.5-mm probes, with resonance frequencies for ^{1}H, ^{13}C, ^{19}F, ^{31}P, and ^{71}Ga of 500.13, 125.77, 470.53, 202.46, and 152.52 MHz, respectively. Typically, $\pi/4$ pulse widths of 2.1 μs, repetition times of 2 s, and spectral widths of 100 kHz were used for single pulse ^{1}H MAS experiments. The MAS speed employed was 30 kHz. The single pulse ^{71}Ga MAS experiment was performed with a pulse length of 1.6 μs corresponding to a soft pulse of $\pi/8$ and a recycle delay of 0.1 s. A Hahn echo sequence was also acquired using selective pulses. The experiment was synchronized with rotation speed (30 kHz), for which an echo delay of 220 μs corresponding to the FID length was set. ^{13}C MAS spectra were acquired using 4-mm ZrO_2 rotor under conditions of both high-power proton decoupling and ^{1}H to ^{13}C cross polarization (CP). The ^{13}C{^{1}H} decoupled spectrum was run with a pulse length of 5.9 μs ($\pi/2$), a repetition delay of 20 s, a rotation rate of 12.5 kHz, and decoupling power of 9 kHz. The ^{13}C{^{1}H} CP experiment was run using the following conditions: spinning rate of 5 kHz, contact time of 1 ms, and relaxation delay of 2 s in Hartman−Hahn conditions. ^{19}F 30 kHz-MAS spectrum was obtained with a 0.7 μs pulse ($\pi/4$) corresponding to a rf power of 175 kHz and 15 s repetition delay. Single pulse ^{31}P MAS, ^{31}P{^{19}F} CPMAS, and ^{31}P-^{19}F HETCOR (CP) experiments were acquired with spinning at a frequency of 30 kHz, 10 kHz, and 20 kHz, respectively. Quantitative conditions were applied for the single pulse experiment using 0.4-μs pulse ($\pi/10$) and 40 s as relaxation delay. Hartman−Hahn condition for the CP was determined on the studied compound. The optimum contact and repetition times were found to be 3 ms and 13 s, respectively. Since the ^{31}P-^{19}F HETCOR sequence was based on a CP sequence, the acquisition conditions were similar to those of the CP experiments. A minimum spinning speed of 20 kHz was found for this experiment in order to get enough resolution in ^{19}F dimension. All spectra were referenced to the chemical shift of adamantane at 1.74 ppm for ^{1}H and 38.3 ppm for ^{13}C, $NH_4Ga(SO_4)_2{\cdot}12H_2O$ at −1.7 ppm for ^{71}Ga,[40] NaF at −221.0 ppm for ^{19}F, $NH_4H_2PO_4$ at 0.0 ppm for ^{31}P relative to standards tetramethylsilane, $Ga(NO_3)_3$ aqueous solution, $CFCl_3$, and H_3PO_4 85 wt % in water, respectively. Decomposition of spectra was achieved using the dm2004 NMR simulation software.[41]

Results and Discussion

Structure Description. The MIL-90 compound exhibits a three-dimensional structure (Figure 1) which is based on the connection of GaO_5X and GaO_2X_4 (X = F or OH) octahedra with GaO_4 and PO_4 tetrahedra and C_2O_4 oxalate groups. There are two distinct crystallographically inequivalent phosphorus atoms P1 and P2, which are in a nearly tetrahedral coordination with typical P−O distances within 1.503(5)−1.549(5) Å. The gallium atoms occupy three crystallographic sites; one of them (Ga3) is located on the special position *1a*. One of the gallium atoms (Ga2) is tetracoordinated to four oxygen atoms with typical Ga−O distances within 1.810(5)−1.831(4) Å. The two other gallium atoms are in octahedral coordination with different surroundings. Ga1 is coordinated to five oxygen atoms and one fluorine/hydroxyl (site F1) group (GaO_5X). The site F1 bridges Ga1 and Ga3. As it will be discussed later through the NMR results, the fluorine position is actually shared with some fraction of the hydroxyl group; fluorine and hydroxyl populations were observed to be 72% and 28%, respectively. Two of these oxygen atoms (O1 and O3) belong to the oxalate group (C1−O1 = 1.242(8) Å, C1−O3 = 1.262(8) Å, C1−C1 = 1.543(12) Å), which acts as a bidentate ligand between two $GaO_5F_x(OH)_{1-x}$ ($x \approx 0.72$) octahedra. It results in a distortion of the GaO_5X octahedron with shorter bond length for the oxygen and fluorine atoms (Ga1−(O,F) = 1.895(5)−1.929(4) Å) and two longer ones for the oxygen atoms belonging to the oxalate ligand (Ga1−O1

(40) Timken, H. K. C.; Oldfield, E. *J. Am. Chem. Soc.* **1987**, *109*, 7669.

(41) Massiot, D.; Fayon, F.; Capron, M.; King, I.; LeCalve, S.; Alonso, B.; Durand, J. O.; Bujoli, B.; Gan, Z.; Hoatson, G. *Magn. Reson. Chem.* **2002**, *40*, 70.

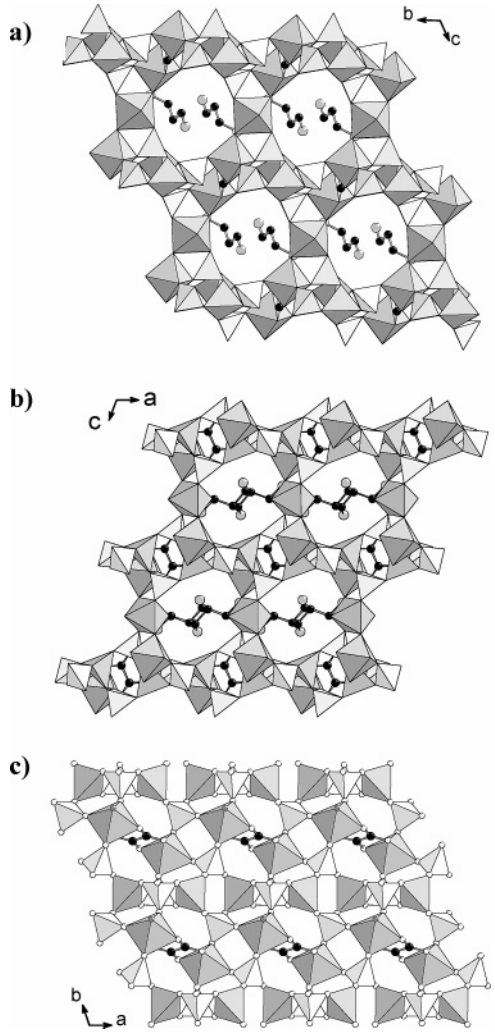

Figure 1. Views of the structure of MIL-90 along [100] (a) and [010] (b) showing the 10-ring channels. Representation of a sheet in the (*a*, *b*) plane indicating the dimer of gallium octahedra linked through the oxalate anion and their connectivities with the PO_4 and GaO_4. White tetrahedra, PO_4; gray polyhedra, GaO_4, GaO_5X, and GaO_2X_4 (X = F or OH). Black circles are the carbon atoms of oxalate species.

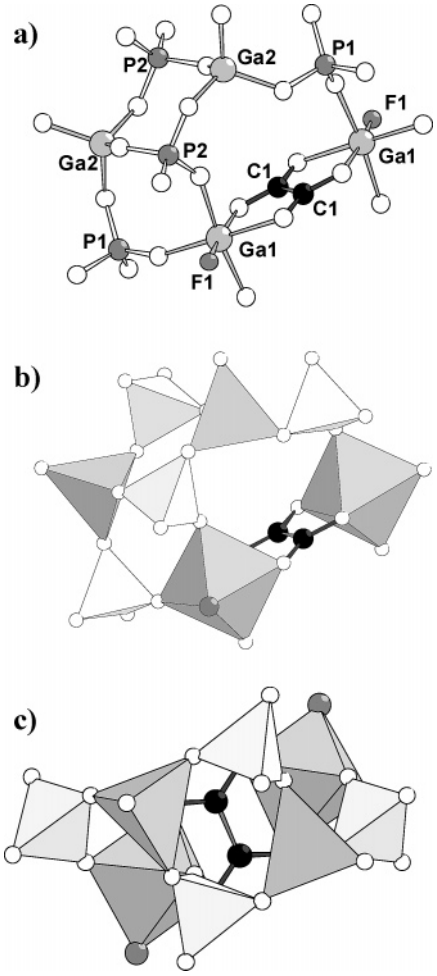

Figure 2. Details of (a and b) the building unit $Ga_4O_5F_2(OH)_2(C_2O_4)(PO_4)_4$ observed in the (001) layer, showing the connectivities between phosphate, oxalate. and gallium polyhedron, and of (c) the building species along the *b* axis showing the stacking of the square unit of 2 GaO_4 and 2 PO_4 tetrahedra and the plane of the oxalate ligand bridging the gallium octahedra GaO_5X (X = OH, F). White tetrahedra, PO_4; gray polyhedra, GaO_4, GaO_5X, and GaO_2X_4 (X = F or OH).

= 2.041(5) and Ga1−O3 = 2.015(5) Å). The last gallium atom Ga3 is coordinated to two oxygen atoms (2 × Ga3−O10 = 1.930(5) Å), two fluorine atoms (2 × Ga3−F1 = 1.958(4) Å), two hydroxyl group (2 × Ga3−O9 = 1.897(5) Å). For this gallium octahedron GaO_2X_4 (X = F or OH), or alternatively $Ga3(O10)_2(F1)_2(O9H)_2$, with the two hydroxyl sites O9H are terminal and are located in a trans position, whereas the fluorine sites F1 bridge the gallium Ga1 and Ga3 together and are in a perpendicular trans position. Here again, both F1 and O9H sites are statistically distributed between fluorine and hydroxyl groups according to the NMR results (see below).

The open framework of MIL-90 is built up from the connection of oxalate-bridging dimers of gallium octahedron $GaO_5F_x(OH)_{1-x}$ ($x \approx 0.72$) linked to the phosphate groups by corner sharing (Figure 2a and b). Each PO_4 unit is also connected to two additional gallium tetrahedra GaO_4 and this forms a square ring of two GaO_4 and two PO_4 moieties (in a strict Ga−O−P alternation), which are stacking with the oxalate ligand along the *b* axis. This results in the formation of a building unit with pseudo-rectangular shape and composition $Ga_4O_5(F_x(OH)_{1-x})_4(C_2O_4)(PO_4)_4$ ($x \approx 0.72$) (Figure 2c). They are connected to each other in the (*a*, *b*) plane (Figure 1c). Within the layer, two adjacent rectangular units are arranged with the same orientation along the *b* axis. The sheets are joined together through the gallium octahedra GaO_2X_4 (X = F or OH) via the fluorine atoms bridging from the dimer of oxalate-$GaO_5F_x(OH)_{1-x}$ ($x \approx 0.72$) octahedra and the remaining free oxygen atoms from phosphate groups. It generates a three-dimensional network with a system of channels running along [010] (Figure 1b) and [100] (Figure 1a). Each type of tunnel is delimited by 10 polyhedra comprising four PO_4 alternating with two groups of GaO_5X and GaO_2X_4 (X = F or OH) octahedra and two GaO_4 species. The estimated size of the tunnels is 4.5 × 4.5 Å (based on an oxygen ionic radius of 1.35 Å). Within the channels is located the 1,3-diaminopropane molecule, which is protonated twice in order to balance the negative charges of the framework. The terminal ammonium groups of the occluded organic molecules preferentially interact with the terminal hydroxyl or fluorine group OH of the GaO_2X_4 (X = F or

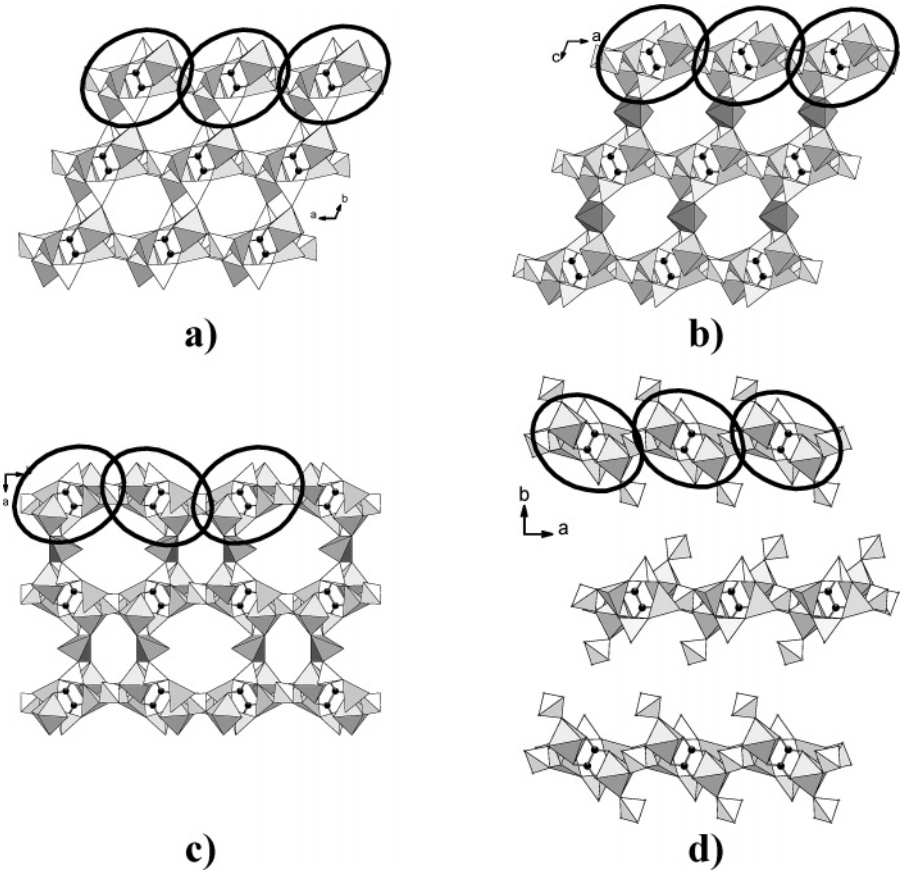

Figure 3. Views of the structures of (a) $K_2Ga_4(C_2O_4)(PO_4)_4{\cdot}2H_2O$,[24] (b) MIL-90 (c) $Ga_5(OH)_2(C_{10}H_9N_2)(C_2O_4)(PO_4)_4{\cdot}2H_2O$[23], and (d) $Ga_4(C_2O_4)(H_2PO_4)(PO_4)_4{\cdot}(R\text{-}C_5H_{14}N_2)_2{\cdot}2H_2O$,[25] showing the various arrangements of the "pseudo-rectangular" building brick (indicated with an open circle). Occluded species (H_2O, K, or amine) are omitted for clarity. Two adjacent building blocks have the same orientation in $K_2Ga_4(C_2O_4)(PO_4)_4{\cdot}2H_2O$ and MIL-90, whereas they have opposite orientation in $Ga_5(OH)_2(C_{10}H_9N_2)(C_2O_4)(PO_4)_4{\cdot}2H_2O$. In $Ga_4(C_2O_4)(H_2PO_4)(PO_4)_4{\cdot}(R\text{-}C_5H_{14}N_2)_2{\cdot}2H_2O$, the structure is lamellar and is based on the connection of building blocks with similar orientation to each other. The occurrence of nonbonded phosphate group prevents any further condensation for making a 3D network.

OH) octahedral units via strong hydrogen bonds ($d_{OH\cdots N1}$ = 2.768(3) and 2.895(1) Å). Other hydrogen bond interaction occurs with some anions of the framework ($d_{O7\cdots N1}$ = 3.052(1), $d_{O11\cdots N2}$ = 2.960(9), and $d_{O2\cdots N2}$ = 2.969(1)).

The occurrence of such a rectangular building brick comprising the dimer of octahedral units linked through the oxalate ligand and square ring of four tetrahedral units was previously reported in other mixed phosphate−oxalate compounds (Figure 3a, c, and d). For instance, a similar layer of rectangular building blocks is encountered in $K_2Ga_4(C_2O_4)(PO_4)_4{\cdot}2H_2O$.[24] The sheets are directly connected to each other through the remaining free atoms of the different polyhedron PO_4, GaO_4, and GaO_6. A second example is found in the gallium-based phosphato−oxalate $Ga_5(OH)_2(C_{10}H_9N_2)(C_2O_4)(PO_4)_4{\cdot}2H_2O$,[23] which exhibits layers of rectangular building unit connected to each other in such a way that two adjacent units have an opposite orientation. The sheets are linked together via the GaO_4N square pyramids units. This type of building unit is also found in the layered gallium phosphate−oxalate $Ga_4(C_2O_4)(H_2PO_4)(PO_4)_4{\cdot}(R\text{-}C_5H_{14}N_2)_2{\cdot}2H_2O$,[25] in which the adjacent building blocks have the same orientation. The occurrence of additional nonbonded phosphate groups pointing up and down the sheet prevents any further condensation for constructing a 3D network.

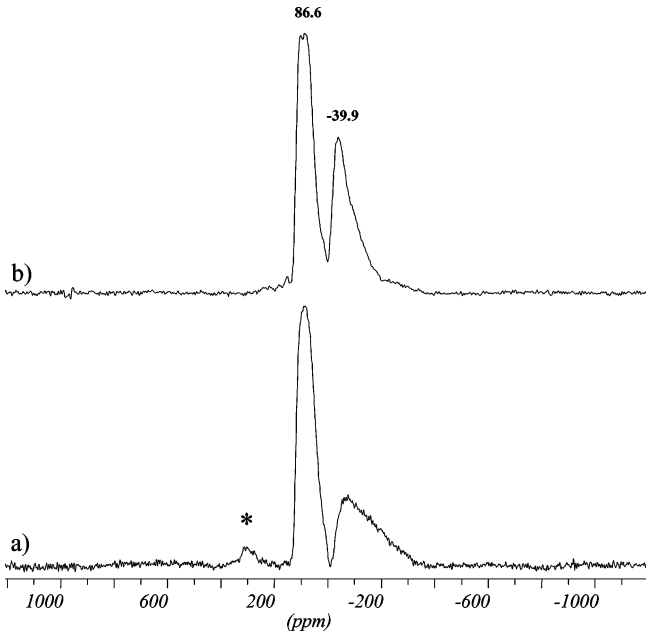

Figure 4. Single pulse (a) and Hahn echo (b) ^{71}Ga MAS NMR spectra of MIL-90 acquired at a spinning speed of 30 kHz. Star denotes satellite sideband and the indicated values correspond to the apparent peak maximal.

NMR Spectroscopy. Single pulse and Hahn echo ^{71}Ga MAS NMR show two components, with their

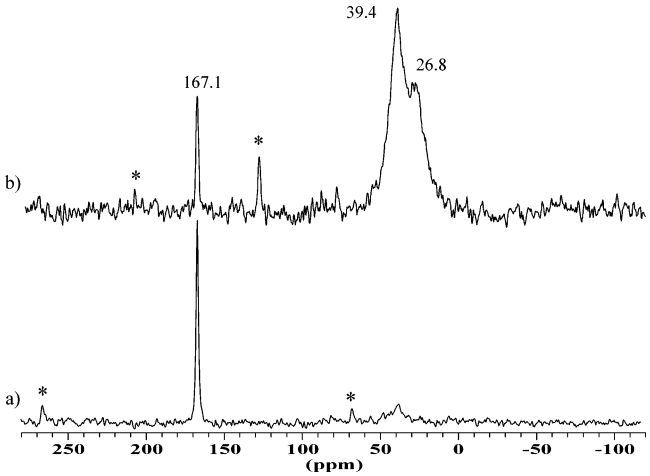

Figure 5. $^{13}C\{^1H\}$ decoupled MAS (a) and CPMAS (b) spectra of MIL-90 acquired at a spinning speed of 12.5 and 5 kHz, respectively. Stars denote satellite sidebands.

maximum intensity at −39.9 and 86.6 ppm, and their apparent chemical shift, with an approximate ratio of 1:1 (Figure 4a and b). A well-established correlation links gallium coordination to their chemical shifts for Ga_{IV}, Ga_V, and Ga_{VI}.[42] The peak at 86.6 ppm is assigned to the tetrahedrally coordinated Ga2. However, only one hexacoordinated gallium site is observed in the Hahn echo NMR experiment. By analogy with the structure published by Hung et al. where just the interlamellar hexacoordinated Ga3 sites are missing compared to this structure, their ^{71}Ga NMR showed the two types of tetra- and hexacoordinated Ga in the expected 1 to 1 intensity ratio.[24] The Ga3 site is therefore not observed due to geometrical distortion. The reasons of lack of perfect symmetrical octahedra are various including the different nature of coordinating atoms, namely O and F, the distribution between F and OH anions, and the preferential H-bond interactions of terminal group with protonated amines. All these effects contribute to the distortion of the environment around the Ga3 site.

The $^{13}C\{^1H\}$ decoupled MAS NMR experiment leads to a very sharp peak at 167.1 ppm due to the oxalate carbons (Figure 5a). This result is consistent with one unique equivalent oxalate carbon site as expected according to diffraction analysis. Signals of occluded organic molecules appear more clearly using a CPMAS sequence (Figure 5b) since cross polarization is more efficient for sites bearing protons. Two broad signals are visible at 26.8 and 38.4 ppm that can be assigned to CH_2 in beta and alpha position of the 1,3-diaminopropane molecule, respectively. The important broadening of these signals compared to the signal of oxalate moieties may indicate statistical disorder of the occluded organic molecules. Chemical shift distribution of different local environments within the pores of the chain molecules may be the main cause of the signal broadening.

The ^1H NMR spectrum of MIL-90 and its decomposition by simulation are displayed in Figure 6. The three resolved signals at $\delta = 2.2$, 3.4, and 7.1 ppm in a 1:2:3 ratio can be assigned to the different types of hydrogen of the diprotonated amine molecule namely CH_2 in beta and alpha, and NH_3, respectively. This result confirms definitively that the organic amine template is fully protonated.

The ^{19}F MAS NMR spectrum of MIL-90 displays a set of lines ranging from −135 to −148 ppm (Figure 7), in contrast with the single crystallographic fluorine site suggested by diffraction analysis (F1). The spectrum can be decomposed by simulation of a main signal at −148.1 ppm with a shoulder at −143.2 ppm, and two other small peaks at −139.4 and −134.8 ppm accounting for 72% (−148.1 ppm and −143.2 ppm together), 12% (−139.4 ppm), and 16% (−134.8 ppm) of the total ^{19}F NMR response. The first signal with a shoulder is assigned to bridging fluorine in F1 site, while the two latter signals are assigned to the O9H site partially substituted by fluorine. This random OH/F distribution in population could not be detected by X-ray diffraction due to the very close electronic configurations it repre-

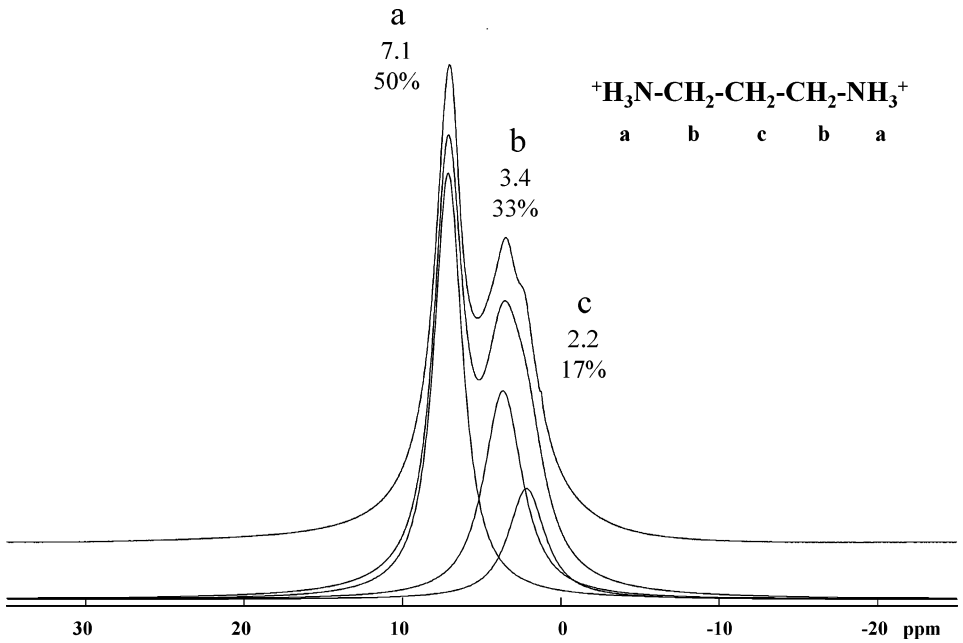

Figure 6. Experimental ^1H MAS NMR spectrum (top) of MIL-90 collected at a spinning speed of 30 kHz. The simulated spectrum and its decomposition are included (bottom).

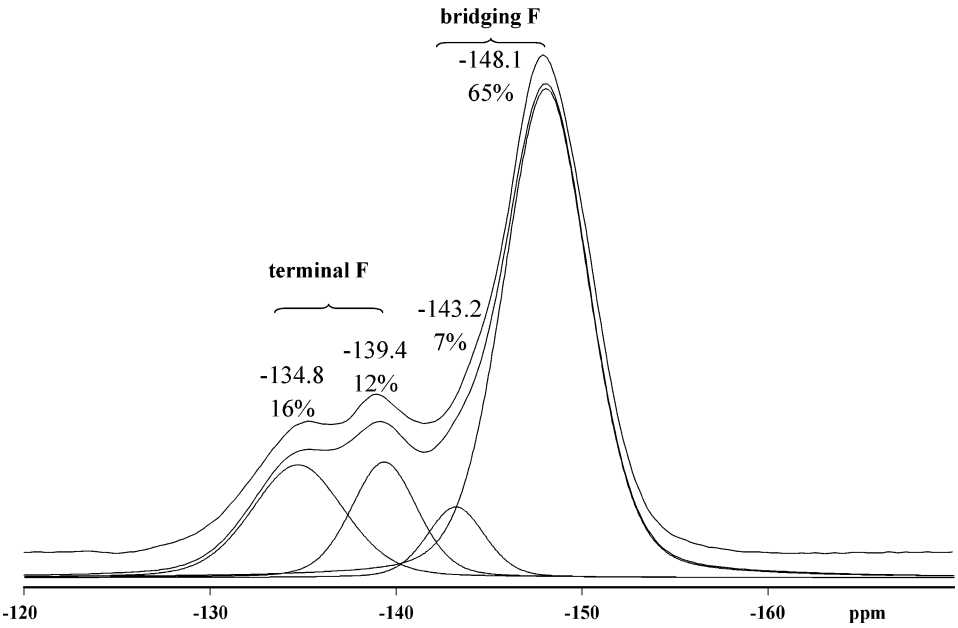

Figure 7. Experimental ^{19}F MAS NMR spectrum (top) of MIL-90 collected at a spinning speed of 30 kHz. The simulated spectrum and its decomposition are included (bottom).

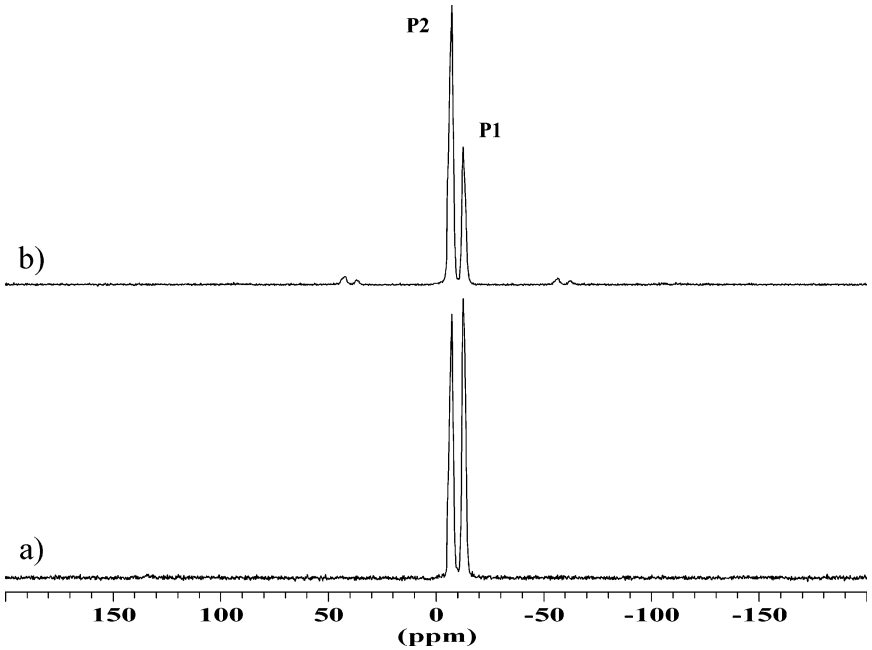

Figure 8. ^{31}P MAS (a) and $^{31}P\{^{19}F\}$ CPMAS (b) spectra of MIL-90 acquired at a spinning speed of 30 and 10 kHz, respectively.

sents. Therefore, the fluorine population of the F1 site is set to ~0.72, whereas it is ~0.28 for the O9H site of the terminal Ga−OH bonding. The hydroxyl NMR signals overlap just in the region of the CH_2 groups and represent only about 10% of the total ^1H NMR signal.

The presence of two crystallographically different phosphorus centers in MIL-90 is confirmed by NMR data. ^{31}P MAS NMR spectrum (Figure 8a) showed two distinct peaks at δ around −7 and −13 ppm in perfect equal population in accordance with the crystallographic data. Usually for microporous fluorinated gallium phosphates, chemical shift values fall in the broad range from 1 to −19 ppm (ref 85% H_3PO_4).[43−45] In a $^{31}P\{^{19}F\}$ CPMAS NMR experiment (Figure 8b) the two signals are observed, but the intensity of the peak at lower field is considerably enhanced relative to the second one. Therefore, the resonance peak located at δ around −7 is attributed to P2, and then −13 is attributed to P1 since the interatomic distances from phosphorus to the closest neighbor fluorine site F1 were 3.3 Å for P2 and 4.2 Å for P1.

A thorough examination of the ^{31}P spectra (see Figure 9) reveals the presence of two additional shoulders for the signal of P2 and one shoulder for P1. These observa-

(42) Massiot, D.; Vosegaard, T.; Magneron, N.; Trumeau, D.; Montouillout, V.; Berthet, P.; Loiseau, T.; Bujoli, B. *Solid State NMR* **1999**, *15*, 159.

(43) Taulelle, F.; Samoson, A.; Loiseau, T.; Férey, G. *J. Phys. Chem. B* **1998**, *102*, 8588.

(44) Reinert, P.; Marler, B.; Patarin, J. *J. Mater. Sci.* **2000**, *35*, 2965.

(45) Matijasic, A.; Paillaud, J.-L.; Patarin, J. *J. Mater. Chem.* **2000**, *10*, 1345.

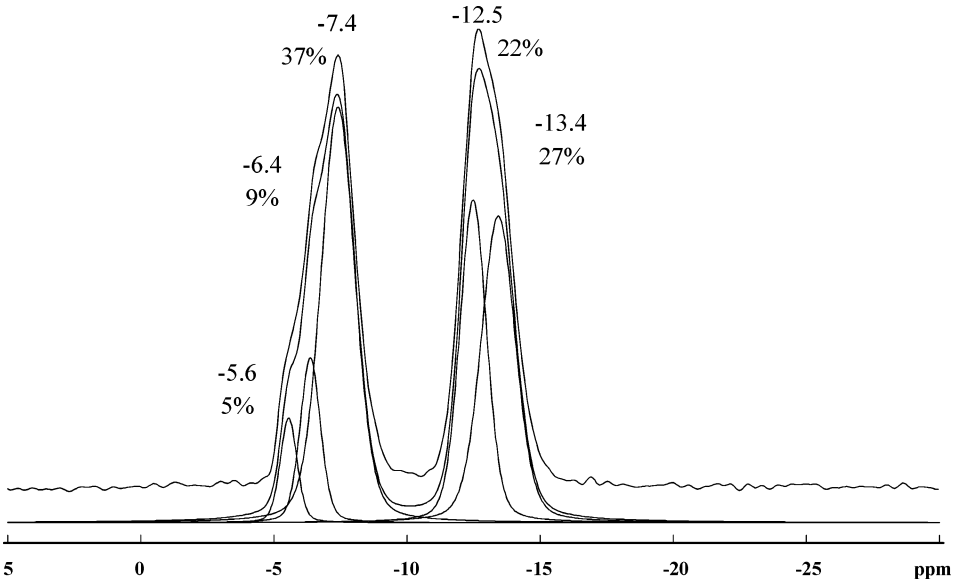

Figure 9. Experimental ^{31}P MAS NMR spectrum (top) of MIL-90 collected at a spinning speed of 30 kHz. The simulated spectrum and its decomposition are included (bottom).

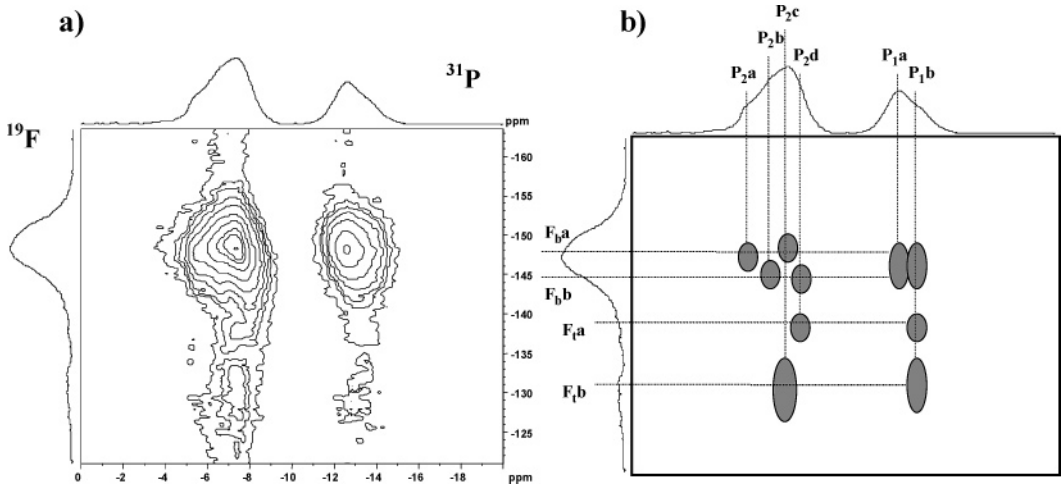

Figure 10. (a) ^{19}F → ^{31}P HETCOR spectrum of MIL-90. The ^{19}F and ^{31}P resonances appear along the vertical and horizontal axes, respectively. Experimental conditions: MAS speed, 20 kHz; CP contact time, 2 ms; delay between scans, 13 s; 128 t_1 values with an increment of 50 μs were used with 16 FIDs for each t_1. (b) Schematic presentation of correlations between sites.

tions could be related to the ^{19}F NMR results with respect to the population distribution between OH and F. Therefore, at least three phosphorus environments exist according to the occupancy of the F1 site or terminal OH sites either by F or OH. Since P2 phosphorus is closer to those sites (F1 and O9) than P1 phosphorus, NMR response for P2 should be more sensitive to this disorder than P1. This is the reason why more resolved signals are observed for P2 signals than for P1 one. Quantitative analysis on the more resolved signal P2 indicates that the signal can be decomposed in three components with a relative proportion of 10%, 18%, and 72% very close to the decomposition of the ^{19}F spectrum into three species with the following proportions: 12%, 16%, and 72%. The presence of several distinguishable phosphorus environments could not be detected by the XRD method, which did not allow the distinction between the different kinds of P1 on one hand and the ones of P2 on the other hand.

Investigating the nature of the distribution of fluorine atoms and hydroxyl groups in the occupancy of the F and OH sites can complement the analysis of disorder on these sites. This can be done by means of a simple HETCOR experiment with a cross-polarization from ^{19}F to ^{31}P during the mixing time. To fix the value of the contact time for the experiment we performed a cross-polarization dynamics experiment incrementing the contact time from 0.05 to 50 ms. Thus, maximum signal is reached for 3 ms at a spinning rate of 20 kHz. The experimental result as well as a picture showing the different correlations for simplicity is included in Figure 10a and b, respectively. The projection in the indirect ^{19}F dimension is similar to the MAS spectrum showing the four components: F_ba, the main peak and its shoulder, F_bb, of the bridging positions and the two additional peaks, F_ta and F_tb, of the terminal positions. In addition, the 2D HETCOR experiment provides higher resolution in the ^{31}P dimension by comparison to the MAS spectrum. Indeed, four components for P2 signal, P_2a, P_2b, P_2c, and P_2d (a new signal not resolved in the MAS spectrum) and two components for P1, P_1a and P_1b, can be distinguished. Since the P2 site is more sensitive to environmental changes around Ga3 than P1, the four situations sensed by P2 are not completely

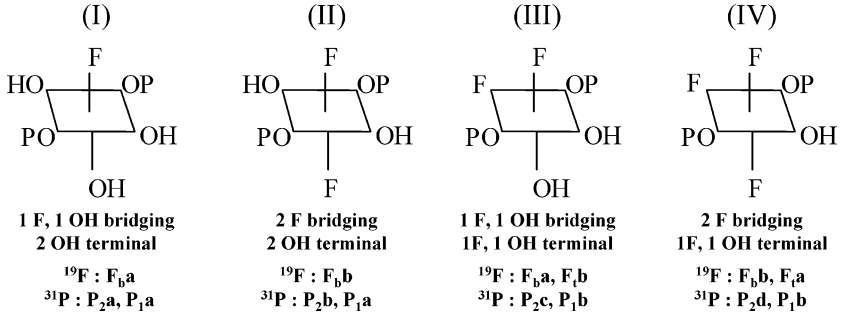

Figure 11. Four different local environments around the octahedral Ga3, GaO_2X_4 (X = F, OH), involving two phosphates (P2), two bridging fluorines (F1), and two terminal hydroxyl groups (O9). The latter two could be partially substituted by OH or F, respectively. The corresponding ^{19}F and ^{31}P NMR signal attribution on the base of the $^{19}F \rightarrow {}^{31}P$ HETCOR spectrum is provided.

distinguished for P1, for which only two situations are resolved. This leads to the assumption that on one hand P_2a and P_2b correspond to the nonresolved P_1a, and P_2c and P_2d correspond to P_1b on the other hand. Therefore, four situations are possible: (I) (P_2a; P_1a); (II) (P_2b; P_1a); (III) (P_2c; P_1b); and (IV) (P_2d; P_1b), as proposed in Figure 11. In the situations I and II, (P_2a; P_1a) and (P_2b; P_1a) correlate with only bridging fluorine F_ba and F_bb, respectively, while in III (P_2c; P_1b) and IV (P_2d; P_1b) correlate with bridging and terminal fluorine (F_ba and F_tb) and (F_bb and F_ta), respectively. This means that in situations I and II the two terminal positions are exclusively occupied by the hydroxyl groups. The difference between the two situations may result in one substitution of terminal fluorine by one hydroxyl. Situation IV implies the substitution of one of the two hydroxyl groups by one fluorine, and for III an additional substitution of the terminal fluorine by one hydroxyl group. These four situations found around the octahedral Ga3, GaO_2X_4(X = F or OH), would suggest six different kinds of hydroxyl (2 + 1 + 2 + 1 in I, II, III, and IV, respectively).

Conclusions

The hydrothermal synthesis of the three-dimensional organic−inorganic mixed framework material MIL-90 or $Ga_5(PO_4)_4(C_2O_4)F_2(OH)_2 \cdot 1.5N_2C_3H_{12}$ and its structural characterization have been described in this work. The compound presents statistical disorder in both the fluorine bridging site and the terminal hydroxyl site shared with OH groups and F atoms, respectively. The structure contains a GaO_2X_4 (X = F or OH) octahedron bearing the two kinds of sites that links sheets, stacked along the *c* axis, to each other. ^{31}P and ^{19}F MAS NMR experiments have probed the distribution of OH and F in these bridging and terminal sites, and assigned the local environments of hydroxyl group and phosphorus nuclei in the framework. The results obtained from the $^{19}F \rightarrow {}^{31}P$ CPMAS experiments not only allow assignment of the two crystallographic phosphorus but also provide the different correlation between ^{31}P and ^{19}F sites with the help of 2D HETCOR experiment. ^{19}F resonances are assigned on the basis of four distinct local environments around the GaO_2X_4 (X = F or OH) octahedra: (I) 1 F, 1 OH bridging and 2 OH terminal; (II) 2 F bridging and 2 OH terminal; (III) 1 F, 1 OH bridging and 1 F, 1 OH terminal; (IV) 2 F bridging and 1 F, 1 OH terminal. ^{1}H and ^{13}C NMR experiments confirm the presence of the occluded 1,3-diaminopropane amine that was difficultly located by diffraction analysis due to the statistical disordering of the molecule. ^{71}Ga MAS NMR indicates the presence of four- and six-coordinated Ga atoms as expected from XRD but the hexacoordinated gallium bridging between layered sheets is undetected due to its distorted environment and to its site distribution with different spheres of coordination.

Acknowledgment. The authors thank Ms. G. Ferriz and Mr. V. Goncalves for their help in the synthesis work.

Supporting Information Available: Crystal data and structure refinement, atomic coordinates and equivalent isotropic displacement parameters, bond lengths and angles, and anisotropic displacement parameters for MIL-90 (txt). Crystallographic information for MIL-90 (cif). This material is available free of charge via the Internet at http://pubs.acs.org.

CM048820O